Microstructure Analysis of Fine Grain Alloy 718 Casting

R. G. Thompson and B. A. Boutwell

University of Alabama at Birmingham

Abstract

Castings with grain size in the range of 50 to 100μ are routinely made using advanced investment casting techniques. This process applied to alloys such as 718 requires heat treatments to homogenize and precipitation harden the alloy. During the casting and heat treatment processes, it is assumed that second phase precipitates such as carbides are beneficial for controlling grain growth but detrimental to mechanical properties. This paper reports on a study to determine the effectiveness of carbides in retarding grain growth. It also examines the effect of the carbides on mechanical properties. Quantitative microstructural techniques were used to make the microstructural measurements and tensile tests were performed for mechanical properties.

Introduction

Investment castings of superalloys such as alloy 718 have been used for many years in radial turbine wheels(1-3). Development of techniques to minimize superheating prior to pouring have resulted in refinement of grain size in the castings(3-6). It is now possible to obtain an equiaxed, ASTM grain size of about 5-6 (55μ) in the casting and about 3-4 (95μ) after final heat treatments(3,4,6,7).

Based on various grain growth and grain boundary pinning theories, it is reasonable to expect that a certain volume of second phase is desirable for retarding grain growth in this process. In alloy 718 two phases, carbide and laves, are present in the cast structure(8-13,24) to facilitate the grain growth control. Both phases however are also expected to compromise mechanical properties(7,14-16). They also getter a large amount of Nb from solution which is suspected of reducing strength by limiting the production of gamma double prime strengthening(10,11,17-23). Thus a tenuous balance might be expected between the benefits of retarding grain growth and the detriments of reduced mechanical properties.

No study has been found in the literature that attempts to quantitatively establish either the detrimental effects of carbide and/or laves on mechanical properties or the beneficial effects of these phases on grain size control. This study was undertaken to do these two things.

Superalloys 718, 625, 706 and Various Derivatives
Edited by E.A. Loria
The Minerals, Metals & Materials Society, 1994

Experimental Procedure and Results

Eight alloy heats of alloy 718 where prepared with the compositions given in Table 1. This composition scheme provided a variable range in C, Nb, Al, and Ti. For each of the eight compositions, four test slabs were cast as per the drawing in Figure 3. A section of the 0.25 inch slab from each chemistry was heat treated to Pratt and Whitney standard PWA 1490 specification. This heat treatment is shown in Table 2.

Microstructure

Typical microstructures of the cast and heat treated material are shown in Figures 2 and 3. It was noted in all cases that the heat treatment fully eliminated the Laves phase from the microstructure as viewed in the light microscope (Figure 1, 2).

Quantitative Microscopy

Carbides

Samples for quantitative microscopy were taken from the top, middle and bottom of each slab as shown in Figure 3. Quantitative microscopy of carbide particles was taken from the as-polished surface of the specimen. The laves phase is softer than the carbides and is not seen on the polished surface. The carbides stand out on the polished surface and are easily counted. A Ziess SEM-IPS system was used with the appropriate filters and background adjustment to count particles larger than about 0.5μ. Spots smaller than this were eliminated. Forty placements per sample were used with the SEM-IPS system.

The results of carbide measurements in the as-cast condition are shown in Tables 3 and 4. The results have been plotted in a number of ways and a correlation was found between carbon concentration and Carbide volume fraction(f_v^C) Correlations were also found between f_v^C and carbide size and heat treatment. It was found that a 60% increase in carbon concentration produced about a 60% increase in carbide volume fraction when measured in the Ziess SEM-IPS system. It was also found that the carbide size grew by 20% and f_v^C increased by 36% during heat treatment.

Quantitative microscopy didn't show a correlation between the carbides and thickness of the test slab or position in the test slab. However, one of the authors visually noted the following correlation between carbide morphology and cooling rate. In the high carbon alloys, the fastest cooling rate (smallest thickness and bottom of mold) produced a preponderance of small spotty carbides. As the cooling rate was reduced, the carbides tended toward a pronounced script morphology. At the slowest cooling rates (largest thickness and top of mold), the carbides appeared to be large and blocky and concentrated on the grain boundaries. The lower carbon alloys showed this transition of carbon morphology to a lesser extend with the tendency not to form a script morphology.

Laves

Quantitative microscopy of the laves phase was performed on samples polished and etched electrolytically in saturated oxalic acid. This treatment reveals both the laves and carbides. Automated counting cannot be used because of etching artifacts and the similar appearance of the phases. In the present evaluation, manual counting in a light microscope was used with the operator selecting the laves phase to count. Both f_v^C (carbide volume fraction) and f_v^L (laves volume fraction) measurements were made with 100 manual placements of a 64 point grid.

A spinoff of this analysis was a comparison between f_v^C obtained using the image analyzer and that obtained manually. This comparison is given in Table 5. It was found that there was a 73% increase for automatic counting over manual counting. It was also found that for manual counting there was almost no difference between counting before etching and counting after etching.

As with carbides, the distribution of laves phase was studied as a function of position in the test slab, composition, cooling rate (slab thickness and position) and heat treatment. The results are shown in Table 3. The results have been plotted in a number of ways and correlations were found between f_v^L and Ti content (Figure 4) and heat treatment. It was found that an increase in Ti content of 60% produced an average 137% increase in laves content. The effect of heat treatment was to dissolve the laves phase completely after the homogenization heat treatment. Although no attempt was made to measure the delta phase, it was noted that some delta precipitation occurred around the laves eutectic. This delta was also dissolved during the homogenization heat treatment.

Grain Size

Grain size was determined using an ASTM grain-size-grid eye piece. This technique requires the operator to visually match a grid to the observed microstructure. Each grid represents a standard ASTM grain size number, graduated in 0.5 of a full number, ie, 6, 5.5, 5, 4.5, etc.. The measured grain sizes are given in Table 6. No correlation was found between grain size and carbide or laves volume fractions. Heat treatment was found to increase grain size.

Mechanical Properties

Hardness Tests

Hardness tests were performed using a microhardness machine. Polished and etched specimen were viewed in the microscope attached to the indentor column. Microhardness was measured in the center of selected grains. The weight and position of the indentation was carefully selected to avoid hitting a grain boundary or carbide particle. In an attempt to determine how many indentations to average per sample, the coefficient of variation was measured for making 10 indentations versus 25 indentations per sample. It was found that the coefficient improved only from 0.4 to 0.3 with increasing the number of indentations, the average hardness changed only 3.7% and the standard deviation was unaffected. Thus it was decided to take 10 indentations per sample.

The hardness values are given in Table 7. It was found that the alloys with extra Al had 25% higher as-cast hardness than their low Al counterparts. Also of interest was the finding that the alloys with extra Ti, Nb and C exhibited the greatest increase in hardness during aging, about 43%. The heats low in these elements showed only 34% increase in hardness with aging. This trend was reversed in the high and low Al heats.

Tensile Test

Tensile test specimen were cut from the 0.5 inch slab of each composition as shown in the drawing of Figure 3. The tensile tests generated yield strength, tensile strength, elongation and reduction in area data.

The results of tensile testing is given in Table 8. The results are most striking in terms of the poor ductility and elongation relative to the extra C content. Another interesting observation is the poor correlation of the microhardness of the heat treated alloys with the yield strength.

Discussion

Grain Size Control

Two issues come to mind immediately relative to grain size control in fine grain castings; one is control of the grain size during solidification and the other is control of grain growth during cooling of the casting and subsequent heat treatment. DTA studies of alloy 718 (8,13,20,24) show that the carbides precipitate during the primary solidification of the matrix while the laves phase precipitates at the end of solidification as a eutectic phase. Furthermore, the carbides and laves phase both appear to be positioned at the grain boundaries suggesting that the carbide is pushed ahead of the solidifying solid interface, thus having no effect on nucleation. From these observations we conclude that the carbides and laves phase have no effect on the solidified grain structure. The effects of these precipitates relative to grain size control is on their role as pinning phases during solid state grain growth.

A Zener pinning model for grain size control would use a relationship between precipitate volume fraction(f), precipitate size(r), and maximum average grain size(D) as follows:

$$D=4r/3f$$

For precipitates like carbides in the size range of 3-5μ, the following volume fractions of precipitates would be required for grain size control in the solid state.

D(μ)	ASTM #	f(%)
45	#6	9 - 15
65	#5	6 - 10
90	#4	4 - 7
127	#3	3 - 5
180	#2	2 - 4

The as-cast microstructures of this study contained 1% - 1.5% carbide and 1% -2% laves. Thus their potential pinning would lead to an average grain size of about 125μ (#3). The actual as-cast grain size of about 90μ (#4) is smaller than the potential maximum grain size predicted by a Zener model.

During heat treatment, grain growth is observed to increase the average grain size from about 90μ to 125μ (#3). The dissolution of the laves phase causes a general decrease in the volume fraction of potential precipitate pinning phase. After the various heat treatments the volume fraction of carbide was measured at between 1 and 2.5%. It is also possible that submicroscopic phases existed along grain boundaries and were not resolved in the quantitative microscopy technique. The small volume fraction of precipitate also made it difficult to count. All of these things taken together suggests a 150μ (#2) to 300μ (#1) grain size from a Zener model. The fact that the grain size was remarkably constant for all samples at about 125μ (#3) suggest one of several possibilities: the grain size has not reached its maximum value and will continue to increase given the opportunity, the Zener model doesn't work well with the small volume fractions observed in these studies, and/or submicron, intergranular precipitates (found to be prevalent in a TEM study of this alloy(10,25,23,19) have a strong effect on grain pinning. Of

these three possibilities, the authors believe that all are equally probable.

The data does suggest that a significant increase in carbon content would be necessary to produce a significant reduction in grain size. For example, as much as 10% carbide might be required to maintain an ASTM #5 grain size. The cost of such a procedure would be a dramatic loss of ductility. On the other hand, it is not obvious that a reduction in carbon content would cause an increase in grain size. Such a reduction in carbon content might pay benefits in increased ductility(7,14,16,27).

Laves Content

The laves content of the as-cast microstructure was found to increase with increased Ti content. The f_v^L, which ranged from about 0.5 to 3.0, was found to dissolve completely during heat treatment. The HIP treatment serves to close microporosity and dissolve the laves phase(11,28,29).

If the casting could be produced without laves present, then it might be possible to reduce or eliminate the HIP/homogenization treatment after casting. It had been suggested in the literature(30,31) that an increased carbon content might reduce the laves content. Presumably this would happen by the carbide using excess Nb and thus "starving" the Nb-rich eutectic from the microstructure. A calculation can be made on how much carbon would be required to "getter" the excess Nb into MC carbides. Microprobe data from Howmet Corporation on fine grain 718 castings similar to those of this study show that the as-cast matrix solubility for Nb is about 3 wgt/o. The excess Nb is the difference between the alloy Nb concentration and the 3 w/o Nb assumed to go into solution. The amount of C (0.08 w/o) used in the present study would only getter about 10% of the excess Nb available for Laves formation in the 5.5 w/o Nb heats. It would take about 3.0 wgt/o C to getter all of the excess Nb from these heats. This indicates that the amount of carbon used in the present study would have little effect on the amount of Nb being segregated into the eutectic laves phase. Consequently the amount of laves present in the as-cast microstructure should not be strongly dependent on the carbon content. This was found to be the case in this study.

Hardness Tests

In examining the microhardness due to Al, it was found that Al accomplished most of its hardening during the casting process. All four heats with extra Al had the highest as-cast hardness. These heats only had a relatively small 34% increase in hardness after heat treatment. However, heats containing extra Ti without extra Al showed more dramatic increases in hardness (60%-70%) following heat treatment. This suggests that there may be potential for replacing some Nb with Ti while still maintaining the alloy's resistance to strain age cracking.

The most striking observation was the lack of correlation of hardness with yield strength or tensile strength.

Tensile Tests

Data from tensile tests at room temperature confirms what might have been expected; increasing the volume fraction of carbide phase decreases ductility. No other relationship was found between microstructure and mechanical properties. The relationship between mechanical properties and microstructure is being studied more closely in another report which is still in progress at this time.

Comparison of Test Slab Data to Production Hardware

Two pieces of Pratt Whitney SSME/AT liquid oxygen preburner flight hardware were cast for comparison to test slab data. The hardware had a variation of cross-sections that spanned the range of thicknesses used in the test slabs. Two chemistries were used in the hardware as given in Table 9. Although these two chemistries are not identical to any of the test slabs, they are reasonably close to experimental chemistries numbers 1 and 8. Data from these two chemistries are also shown in Table 9 for comparison to the hardware. Data that was collected on the hardware included tensile strength(UTS), 0.02 offset yield strength(YS), percent elongation(EL), percent reduction in area(RA), ASTM grain size, carbide volume fraction(f_v^C), Laves volume fraction(f_v^L), and microhardness.

The results suggest that the test slabs give very good information on microstructure and properties of potential production hardware. The data for hardware item #2 and test heat #8 are remarkably similar in most respects. The results for hardware item # 1 and heat # 1 are not quite so close but are still very similar. It appears from these experiments that the test slabs are reliable simulations of production hardware. Furthermore, the trends that were seen in the test slabs such as increased strength with Ti and Nb were transferred to the production hardware. Thus the performance trends found in test slab data serve as reliable indicators of hardware performance.

Conclusions

Fine grain castings of alloy 718 are dependent on their nucleation and growth in the liquid-solid state for their fine grain size. The role of precipitate pinning in controlling grain size in the solid state is relatively independent of the volume fraction of precipitates present in commercial alloy 718. If further advances are to be made in grain refinement, they must be made in the nucleation process.

The dependence of tensile strength on $Ni_3Nb(\gamma'')$ strengthening in alloy 718 is well known. The ability to maximize Nb concentration in solution so that it is available for strengthening is hampered by segregation during casting. Higher strengths and reduced homogenization treatments will only be obtained through alloy modifications which increase the Nb solubility or substitute other strengthening phases.

An approach to increasing the strength of alloy 718 type compositions while maintaining or improving ductility must reduce Nb segregation and reduce f_v^C. This approach is self consistent since reducing Nb segregation would eliminate the need for homogenization treatments. Without a significant homogenization treatment, there would be no need for carbides for grain size control.

Quantitative microscopy of alloys like 718 is difficult because of the small volume fraction of phases and the need to correctly identify each precipitate. Operator bias will produce over counting due to a natural desire to "find" something. This tendency can be reduced in image analysis systems where the results are less dependent on operator bias. Because the laves phase must be counted on the etched surface, highly trained operators are required. A check of the investigator accuracy for both laves phase and carbide phase can be made by comparing the f_v^C value obtained on the polished surface to that obtained on the etched surface.

Acknowledgements

The authors would like to thank Y. Shen and P. Scarber for their would on image analysis. The authors also thank Jan Lane and Roger Dunham of Howmet, and the Rocketdyne Division of Rockwell for their support. This paper was prepared with the support of the Department of Energy on Cooperative agreement No. DE-FC07-921D13163. However, any opinions, findings, conclusions, or recommendations expressed herein are those of the authors and do not necessarily express the views of the DOE.

References

1. A. H. Jones, "An Overview of Alloy 718 in large Structural Castings," Superalloy 718 Metallurgy and Applications, E. A. Loria, TMS, 1989, pp. 307-318.
2. O. W. Balloy and M. W. Coffey, "History of Cast Inco 718," Superalloys 1988, D. N. Duhl, TMS, 1988, pp. 469-474.
3. B. A. Ewing and K. A. Green, "Polycrystalline Grain Controlled Castings for Rotating Compressor and Turbine Components," Supercooling 1984, Maurice Gell, etal., TMS, 1984, pp. 33-42.
4. L. A. James, "Fatigue Crack Propagation in Alloy 718: A Review," Superalloy 718 Metallurgy and Applications, E. A. Loria, TMS, 1989, pp. 499-516.
5. M. Woulds and H. Benson, "Development of a Conventional Fine Grain Casting Process," Supercooling 1984, Maurice Gell, etal., TMS, 1984, pp. 3-12.
6. J. R. Brinegar, L. F. Norris, and L. Rozenberg, "Microcast-X Fine Grain Casting-A Progess Report," Supercooling 1984, Maurice Gell, etal., TMS, 1984, pp. 23-32.
7. G. K. Bouse and M. R. Behrendt, "Mechical Properties of Microcast-X Alloy 718 Fine Grain Investment Castings," Superalloy 718 Metallurgy and Applications, E. A. Loria, TMS, 1989, pp. 319-328.
8. M. J. Cieslak, G. A. Knorovsky, T. J. Headley, A. D. Romig, Jr., " The Solidification Metallurgy of Alloy 718 and Other Nb-Containg Superalloys," Superalloy 718 Metallurgy and Applications, E. A. Loria, TMS, 1989, pp. 59-68.
9. G. K. Bouse, "Application of a Modified Phase Diagram to the Production of Cast Alloy 718 Components," Superalloy 718 Metallurgy and Applications, E. A. Loria, TMS, 1989, pp. 69-77.
10. R. G. Carlson and J. F. Radavich, "Microstructual Characterization of Cast 718," Superalloy 718 Metallurgy and Applications, E. A. Loria, TMS, 1989, pp. 79-96.
11. J. F. Radavich, "The Physical Metallurgy of Cast and Wrought Alloy 718," Superalloy 718 Metallurgy and Applications, E. A. Loria, TMS, 1989, pp. 229-240.
12. D. D. Wegman, "Compositonal Control and Oxide Inclusion Level Comparison of Pyromet 718 and A-286 Ingots Electroslag Remelted Under Air vs. Argon Atmosphere," Superalloys 1988, D. N. Duhl, TMS, 1988, pp. 427-436.
13. W. D. Cao, R. L. Kennedy, and M. P. Willis, "Differential Thermal Analysis (STA) Study of The Homogenization Process in Alloy 718," Superalloys 718,625 and Various Derivations, E. A. Loria, TMS, 1991, pp. 147-160.
14. J. M. Moyer, "Extra Low Carbon Alloy 718," Supercooling 1984, Maurice Gell, etal., TMS, 1984, pp. 443-454.
15. J. J. Schirra, R. H. Caless, and R. W. Hatala, "The Effects of Laves Phase on the Mechnical Properties of Wrought and Cast + HIP Unconel 718," Superalloys 718,625 and Various Derivations, Edward A. Loria, TMS, 1991, pp. 375-388.

16. W. J. Mills, "Effect of Microstructural Variations on the Fracture Toughness of Wrough Alloy 718," Superalloys 718,625 and Various Derivations, Edward A. Loria, TMS, 1991, pp. 573-588.
17. G. Chen, Q. Zhu, D. Wang, X. Xie, and J. F. Radavich, "Effects of Magnesium on Niobruim Segregation and Impact Toughness in Cast Alloy 718," Superalloy 718 Metallurgy and Applications, E. A. Loria, TMS, 1989, pp. 545-552.
18. S. M. Jones, J. F. Radavich, S. Tian, "Effects of Compostion on Segregation Microstructures and Mechanical Properties of Cast Alloy 718," Superalloy 718 Metallurgy and Applications, E. A. Loria, TMS, 1989, pp. 589-598.
19. G. Sjoberg and N. G. Ingesten, "Grain Boundary ?-phase Morphologies, Carbides and Notch Rupture Sensistivity of Cast Alloy 718," Superalloys 718,625 and Various Derivations, Edward A. Loria, TMS, 1991, pp. 603-620.
20. U. Heubner, M. Kohler and B. Prinz, "Determination of the Solidification Behaviour of Some Selected Superalloys," Superalloys 1988, D. N. Duhl, TMS, 1988, pp. 437-448.
21. Z. Yaoxiao, Z. Shunnan, X. Leying, B. Jing, H. Zhuangqi and S. Changxu, "Superalloys with Low Segregation," Superalloys 1988, D. N. Duhl, TMS, 1988, pp. 703-712.
22. X. Xie, Y. Zhang, Z. Xu, K. Ni, Y. Zhu. T. Zhang, Y. Tong, X. Ning, S. Zhang, and J. F. Radavich, "Effect of Oxygen, Nitrogen, and Magnesium on Segregation, Solidification and Mechanical Properites in Alloys 718,"Superalloys 718,625 and Various Derivations, E. A. Loria, TMS, 1991, pp. 241-250.
23. M. G. Burke and M. K. Miller, "Precipitation in Alloy 718: A Combined AEM and APFIM Investigation," Superalloys 718,625 and Various Derivations, Edward A. Loria, TMS, 1991, pp. 337-350.
24. C. Chen, R. G. Thompson, and D. W. Davis, "A Study of Effects of Phosphorus, Sulfur, Boron and Carbon on Laves and Carbide Formation in Alloy 718," Superalloys 718, 625 and Various Derivatives, Edward A. Loria, TMS, 1991, pp. 81-96.
25. A. Oradei-Basile and J. F. Radavich, "A Current T-T-T Diagram for Wrought Alloy 718," Superalloys 718, 625 and Various Derivations, Edward A. Loria, TMS, 1991, pp. 325-335.
26. G. Muralidharan, R. G. Thompson, and S. D. Walck, "Analysis of Precipitation in Cast Alloy 718," Ultramicroscopy 29, North-Holland, Amsterdam, 1989, pp. 277-283.
27. T. Banik, P. W. Keefe, G. E. Maurer, and L. Petzold, "Ultra Fine Grain/Ultra Low Carbon 718," Superalloys 718,625 and Various Derivations, Edward A. Loria, TMS, 1991, pp. 913-924.
27. J. W. Brooks and P. J. Bridges, "Metallurigical Stability of Inconel Alloy 718," Superalloys 1988, D. N. Duhl, TMS, 1988, pp. 33-42.
28. R. E. Painter and J. M. Young, "Liquid Metal Treatments to Reduce Mcroporosity in Vacuum Cast Nickel Based Superalloys," Superalloys 1988, D. N. Duhl, TMS, 1988, pp. 417-426.
29. P. Siereveld, J. F. Radavich, T. Kelly, G. Cole and R. Widmer, "Effect of HIP Parameters on Fine Grain Cast Alloy 718," Superalloys 1988, D. N. Duhl, TMS, 1988, pp. 459-468.
30. B. Radhakrishnan and R. G. Thompson, "A Phase Diagram Approach to Study Liquation Cracking in Alloy 718," Metallurgical Transactions A, Volume 22A, April, 1991, pp. 887-902.
31. B. Radhakrishnan and R. G. Thompson, "Solidification of the Nickel-Base Superalloy 718: A Phase Diagram Approach," Metallurgical Transactions A, Volume 20A, December, 1989, pp. 2866-2868.

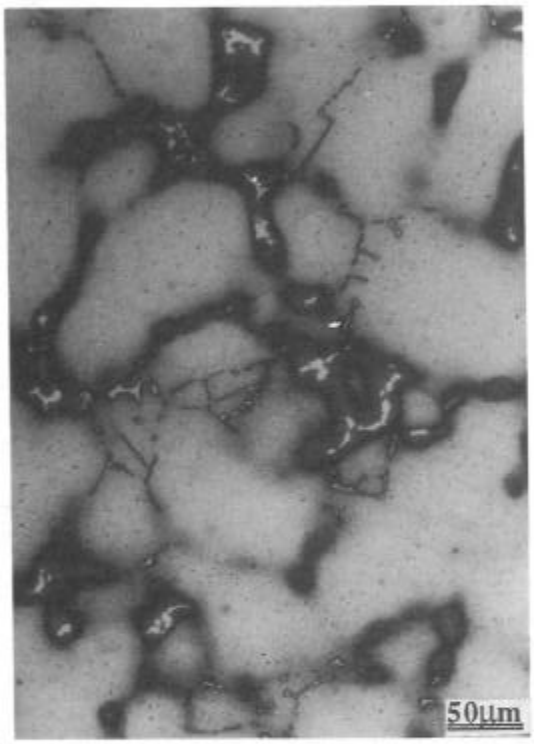

A. As-cast 1.25 in. slab

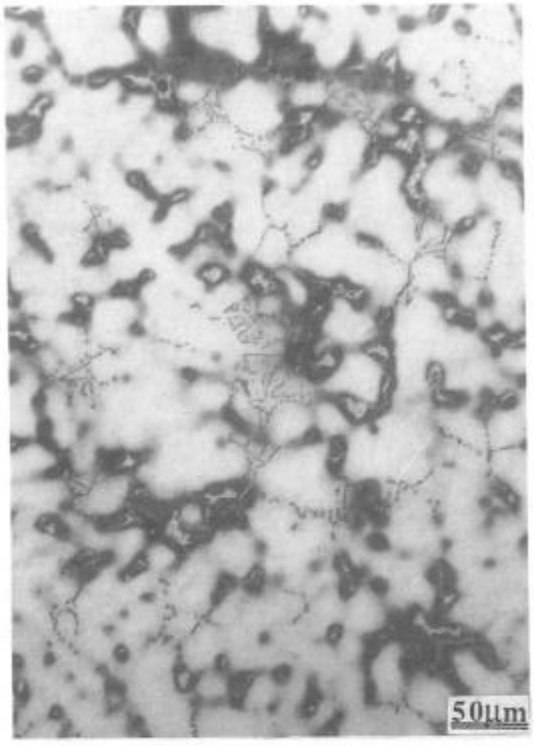

B. As-cast 0.25 in. slab

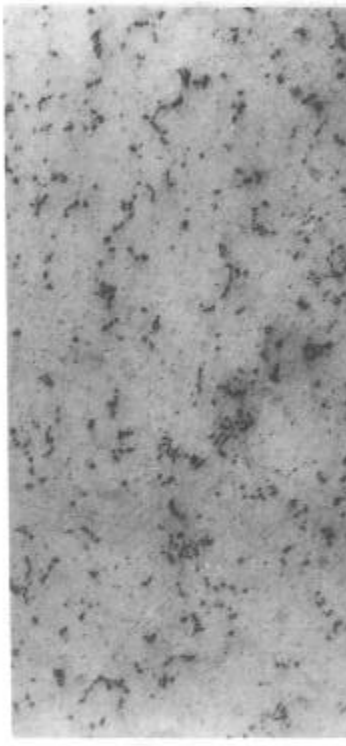

C. Fully Heat Treated 0

Figure 1. Heat 8 Microstructures.

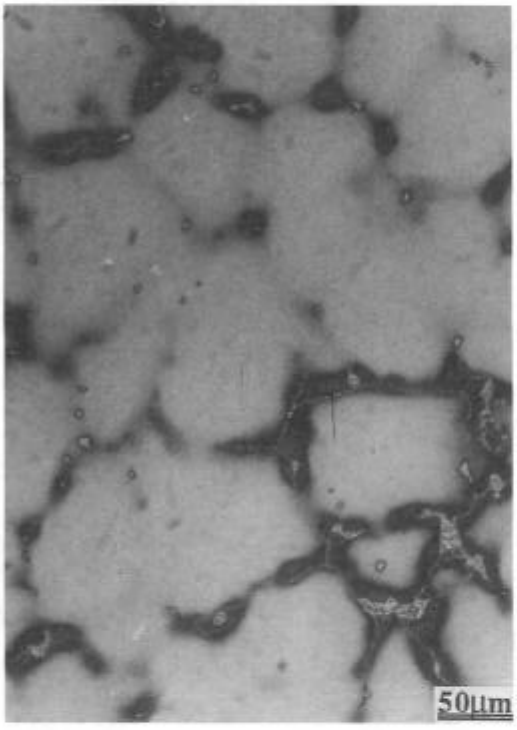

A. As-cast 1.25 in. slab

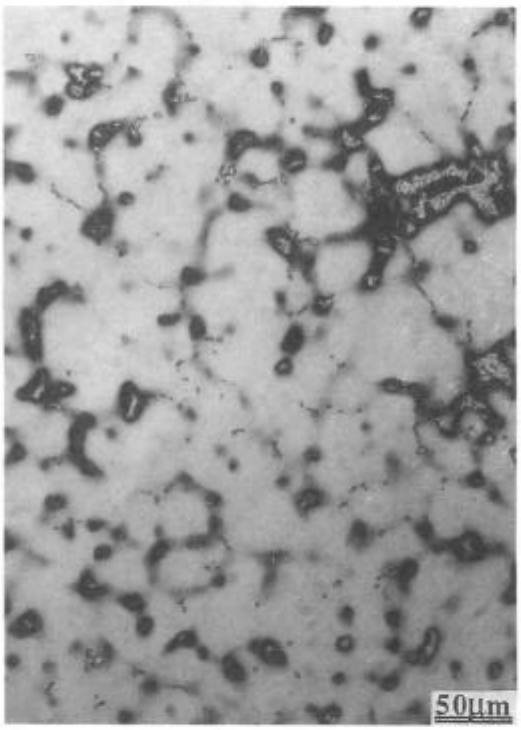

B. As-cast 0.25 in. slab

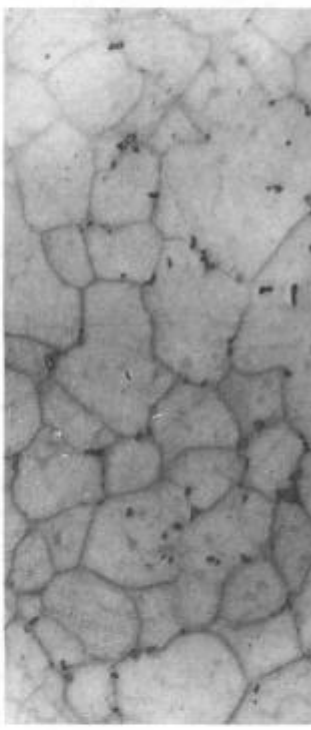

C. Fully Heat Treated

Figure 2. Heat 11 Microstructures.

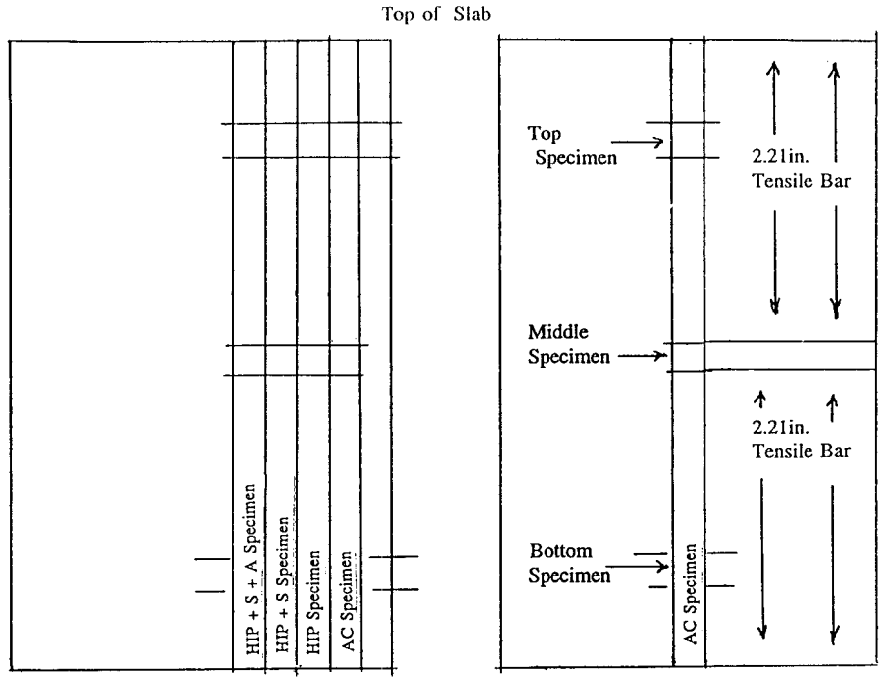

FIGURE 3. Experimental Test Slab Configuration

(Slabs are 3in. X 6in., slices taken from slabs are all 0.25in. wide, top of slab defined by casting gate location with gravity feed from top.)
AC is as-cast, HIP hot isostatic press, S solution, A aged

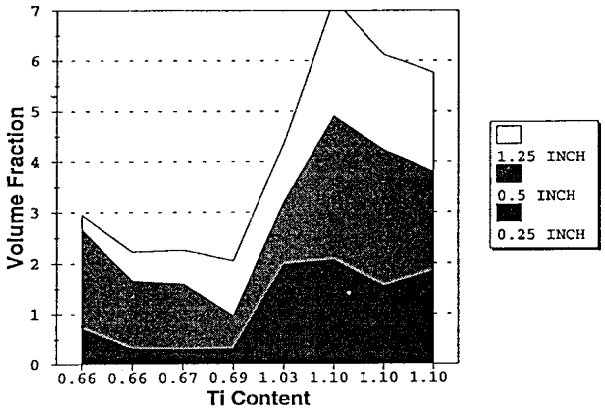

FIGURE 4. AS CAST LAVES FRACTION

TABLE 1

Heat Chemistries (weight percent, w/o)

		Heat Numbers							
Element	Master Heat	1	2	4	8	9	10	11	12
Al	0.47	0.44	0.44	0.45	0.76	0.48	0.76	0.75	0.74
Ti	0.69	0.69	0.66	1.10	1.10	1.03	0.67	0.66	1.11
Cb(+Ta)	4.82**	5.01	5.68	5.60	5.64	4.91	5.00	5.60	4.96
C	0.50	0.05	0.08	0.05	0.08	0.08	0.09	0.05	0.05
Ni	51.75	51.76	51.20	51.30	50.97	51.49	51.23	51.06	51.16
Cr	17.29	17.26	17.17	16.93	16.89	17.20	17.32	17.15	17.17
Fe*	Bal	21.43	21.41	21.22	21.22	21.44	21.54	21.38	21.43
Mo	3.02	3.02	3.02	3.00	3.00	3.01	3.04	3.00	3.03
B	0.004	0.004	0.004	0.004	.004	0.004	0.004	0.004	0.003
Mg	0.0048	<0.001	<0.001	<0.001	<0.001	<0.001	<0.001	0.002	<0.001
Si	0.01	0.02	0.02	0.03	0.02	0.03	0.03	0.03	0.03
Co	0.32	0.28	0.28	0.28	0.28	0.29	0.28	0.28	0.28
Zr	<0.01	0.01	0.01	0.01	0.01	0.01	0.01	0.01	0.01
P	0.002	.002	0.003	0.003	0.003	0.003	0.003	0.003	0.003

* Fe from subtraction of analyzed elements.
** Cb vendor chemistry = 4.75 wt. % (Ta = 0.07 wt. %).

TABLE 2

Heat Treatment

AC	as-cast
HIP	2050°F at 15,000 PSI for 4 hrs.
HIP+S	HIP + 2000°F for 1 hr. and cool at 40°F/min. to below 1000°F
HIP+S+A	HIP + S + 1350°F for 8 hrs. and cool at 100°F/hr. to 1225°F and hold for 8 hrs.

* HIP+S+A is PWA 1490 heat treatment without pre-HIP homogenization.

TABLE 3
VOLUME FRACTIONS
(Standard Deviation Approximately ± 0.35%)

Carbide Volume Fractions
(all thickness, all heats, all positions)

	AS - CAST					HIP+SA+A
	Slab Thickness					0.25"
HEAT #	1.25"	0.75"	0.50"	0.25"	AVERAGE	AVERAGE
1	1.01	0.89	0.87	0.87	0.91	1.06
2	1.49	1.53	1.45	1.27	1.43	1.26
4	0.96	0.93	0.94	0.82	0.91	1.35
8	1.57	1.54	1.21	1.19	1.38	2.28
9	1.53	1.50	1.30	1.22	1.39	2.15
10	1.52	1.05	1.15	1.29	1.25	1.12
11	0.77	0.81	0.76	0.71	0.76	1.19
12	0.73	0.94	0.86	0.85	0.85	1.70
Avg. Low C	0.87	0.89	0.86	0.81	0.86	1.33
Avg. High C	1.53	1.41	1.28	1.24	1.36	1.70

Laves Volume Fractions
(three thicknesses, all heats, only middle position)

	Slab Thickness				
HEAT #	1.25	0.75	0.50	0.25	Average
1	1.09	NA	0.64	0.32	0.68
2	0.28	NA	1.94	0.73	0.98
4	1.97	NA	2.67	1.56	2.07
8	2.33	NA	2.83	2.07	2.41
9	1.15	NA	1.23	1.98	1.45
10	0.66	NA	1.31	0.29	0.75
11	0.57	NA	1.34	0.32	0.74
12	1.89	NA	1.94	1.85	1.89
Avg. High Ti	1.84	0.00	2.17	1.87	1.96
Avg. Low Ti	0.65	0.00	1.31	0.42	0.79
Average	1.24	0.00	1.74	1.14	1.37

* Average low C is the average for the low C heats (1, 4, 11, 12).
Average high C is the average for the high C heats (2, 8, 9, 10).
Each bar thickness is the average of the top, middle, and bottom positions.

TABLE 4

CARBIDE SIZE (microns)*
(Standard Deviation Approximately ± 2.0μ)

	AS - CAST					HIP+SA+A
	Slab Thickness					0.25"
HEAT #	1.25"	0.75"	0.50"	0.25"	AVERAGE	AVERAGE
1	3.51	2.07	3.67	3.36	3.15	3.90
2	4.43	3.62	3.09	2.84	3.50	4.01
4	4.30	4.17	3.95	4.67	4.27	4.28
8	4.37	4.03	3.16	3.02	3.65	4.30
9	3.62	1.24	1.03	1.47	1.84	4.17
10	3.33	3.09	2.80	2.92	3.04	3.74
11	4.64	4.35	3.87	3.61	4.12	4.25
12	3.99	3.95	3.50	3.00	3.61	4.38
Avg. Low C	4.11	3.64	3.75	3.66	3.79	4.20
Avg. High C	3.94	3.00	2.52	2.56	3.00	4.06

* Average low C is the average for the low C heats (1, 4, 11, 12).
* Average high C is the average for the high C heats (2, 8, 9, 10).
* Each bar size is the average of the top, middle and bottom sections of the bar.

TABLE 5

Comparison of QM Data from Different Techniques

			Before Etch (Carbides)			After Etch (Manual)	
Heat #	Thickness	Position	Manual	Auto A	Auto B	Laves	Carbide
1	0.5"	Middle	0.50	0.89	0.92	0.64	0.38
2	0.5"	Middle	1.11	1.47	1.13	1.94	0.95
4	0.5"	Middle	0.34	1.00	0.76	2.67	0.64
8	0.5"	Middle	0.69	1.25	1.11	2.83	0.78
9	0.5"	Middle	0.41	1.36	0.97	1.23	0.38
10	0.5"	Middle	0.52	1.43	0.97	1.31	0.41
11	0.5"	Middle	0.33	0.79	0.79	1.34	0.45
12	0.5"	Middle	0.34	0.97	0.69	1.94	0.44

TABLE 6
Grain Size (ASTM #)

Heat #	AC	HIP	HIP+S	HIP+S+A
1	5	4	4	3
2	5	4	3	3
4	6	4	3	3
8	5	4	4	3
9	6	4	4	3
10	6	4	3	3
11	6	4	3	3
12	5	4	4	3

TABLE 7
Vickers Hardness of the Matrix
(Typical Standard Deviation ~ 30)

	As - Cast	As - Cast (Avg. for all thicknesses)			Full Ht Trtmt	
Heat	0.5" Thcknss	Top	Middle	Bottom	0.25" Thcknss	
	Middle				Middle	% Increase
1	201				232	15
2	211				277	31
4	204				325	59
8	280				380	36
9	221				376	70
10	251				355	41
11	232				340	47
12	277	307	260	285	320	16
Avg. High Al	260				349	34
Avg. Low Al	209				303	45
Avg. H Ti, H Nb, H C	239				343	43
Avg. L Ti, L Nb, L C	230				309	34

TABLE 8

Room Temperature Tensile Properties

	PSI x 10^3			Percent	
Heat #	UTS	0.2% YS	0.02% YS	% El	% RA
1	177	152	123	20	25
2	181	159	136	9	16
4	194	175	153	14	21
8	181	157	125	14	20
9	173	149	132	15	20
10	159	130	108	15	17
11	179	152	134	19	23
12	177	147	121	21	24

TABLE 9
Comparison of Test Slab to Hardware
(Full Heat Treatment)

	Chemistry A (see Table 1)		Chemistry B (see Table 1)	
Control Element	Test Slab #1	Hardware #1	Test Slab #8	Hardware #2
Al	0.44	0.55	0.76	0.40
Ti	0.69	0.95	1.10	1.16
Cb	5.01	4.80	5.64	5.22
C	0.05	0.04	0.08	0.07
Mechanical Properties (PSIx10^3)				
UTS	179-176	161-164	176-185	178-185
YS	150-153	134-138	150-160	160-166
EL	19-20	21-27	12-17	9.2-12.5
RA	23-26	25-34	19-23	16.2-22.6
Grain Size (ASTM) (Typical Section)				
	3	2	3	4
Carbide Values (Typical)				
Volume	1.06 (± 0.3%)	NA	2.28	1.65
Size	3.9 (± 2.0μ)	NA	4.3	6.0
Laves				
	None	None	None	None
Hardness (Vickers) (Typical Section)				
	325	NA	329	450